Journal of Reinforced Plastics and Composites
http://jrp.sagepub.com/

Progressive Failure of Laminated Composites with a Hole under Compressive Loading

Seng C. Tan and Jose Perez

Journal of Reinforced Plastics and Composites 1993 12: 1043
DOI: 10.1177/073168449301201002

The online version of this article can be found at:
http://jrp.sagepub.com/content/12/10/1043

Published by:
SAGE
http://www.sagepublications.com

Progressive Failure of Laminated Composites with a Hole under Compressive Loading

SENG C. TAN*
Wright Materials Research
P.O. Box 31667
Dayton, OH 45437

JOSE PEREZ
Stanford University
Linear Accelerator Center
P.O. Box 4349
Stanford, CA 94309

ABSTRACT: A progressive failure model that was developed earlier for tensile loading is extended for laminated composites under uniaxial compressive loading. This model is capable of predicting the extent of damage at any load level, the stiffness loss, the stress-strain behavior and the residual strength of the laminates. The model is composed of the stress analysis, the failure analysis and a degradation model for the damaged lamina. Comparison with three sets of experimental data shows that good correlation was obtained between the theoretical prediction and the data for the ultimate strength. The predicted micro-damage includes matrix cracking and fiber breakage (shear crippling or microbuckling) that agrees reasonably well with the experimental X-ray radiograph.

1. INTRODUCTION

COMPRESSIVE RESPONSE IS one of the key parameters that is used in the design of composite structures. Since most structures contain fastener holes, the compressive response of composite structures with a cutout requires attention and study. The existing studies include strength prediction models, experimental study of the failure mechanisms around the hole and failure prediction using a progressive model. They are described with more detail in the following.

Compressive strength of laminated composites containing an open hole has been predicted with reasonably good accuracy using semi-empirical models. These include average stress failure model [1], point stress failure model [2] based on the work of Whitney and Nuismer, minimum strength model in con-

*Author to whom correspondence should be addressed.

junction with a first-ply-failure criterion [3], and effective average stress and minimum strength models in conjunction with a first-ply-fiber-failure criterion [4]. They all use a characteristic length to absorb the micro-damage near the hole. Closed form solutions can generally be obtained for this class of approaches.

To predict the extent of damage and damage progression in composites, we need to use progressive failure models. This class of approaches includes Nuismer [5], Chou, Opringer and Rainey [6], Irvine and Ginty [7], Tan [8] and Chang and Lessard [9]. The majority of these approaches deal with tensile loading. However, it is expected that most of them could be extended to predict the structural response under compressive loading. The accuracies of the modified models are uncertain before being examined with experimental results.

More experimental work has been devoted to studying the damage mechanisms around the hole under compressive loading rather than tensile loading. The results [10–15] all agree that shear crippling or microbuckling is the failure mode initiated from the hole. Visually, this shear crippling or microbuckling appears like a crack emanating from the hole. It grows as the applied load increases.

2. FORMULATION OF THE PROBLEM

Consider a composite laminate loaded by the in-plane compressive loading $\bar{\sigma}_x$ and containing a central hole, as shown in Figure 1, where $2a$ and W denote the hole diameter and plate width, respectively. Assume the laminate is symmetric with respect to its mid-plane so that there is no coupling between the extensional and the bending moment. Under this circumstance, the constitutive relations of an anisotropic undamaged lamina, in the laminate axes, can be written as

$$\begin{Bmatrix} \sigma_x \\ \sigma_y \\ \tau_{xy} \end{Bmatrix} = \begin{bmatrix} Q_{11} & Q_{12} & Q_{16} \\ Q_{12} & Q_{22} & Q_{26} \\ Q_{16} & Q_{26} & Q_{66} \end{bmatrix} \begin{Bmatrix} \epsilon_x - \epsilon_{xN} \\ \epsilon_y - \epsilon_{yN} \\ \gamma_{xy} - \gamma_{xyN} \end{Bmatrix} \tag{1}$$

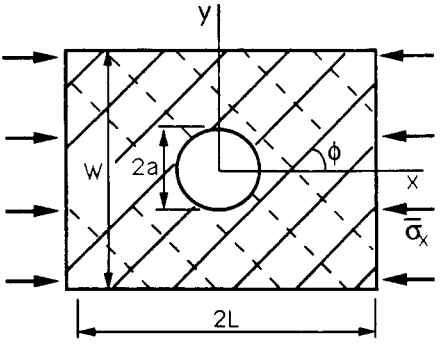

Figure 1. *A composite laminate with a hole subjected to uniaxial compression.*

where σ_x, σ_y, τ_{xy} are the lamina stresses; Q_{ij}, $i,j = 1,2,6$ are the lamina stiffnesses; ϵ_x, ϵ_y, γ_{xy} are the total strains, and ϵ_{xN}, ϵ_{yN} and γ_{xyN} are the nonmechanical strains or initial strains. The off-axis stiffnesses Q_{ij} can be expressed in terms of on-axis stiffnesses C_{ij}, which are given in engineering properties E_{11}, E_{22}, G_{12} and ν_{12}. The relations between Q_{ij} and C_{ij} can be found in any standard textbook. The transformation of the nonmechanical strains between the principal material axes and the laminate axes can be found in Reference [8].

3. FINITE ELEMENT ANALYSIS

The stress analysis was performed on the x-y plane. Each element is governed by the following stress-strain relations

$$\begin{Bmatrix} \bar{\sigma}_x \\ \bar{\sigma}_y \\ \bar{\tau}_{xy} \end{Bmatrix} = \begin{bmatrix} \bar{A}_{11} & \bar{A}_{12} & \bar{A}_{16} \\ \bar{A}_{12} & \bar{A}_{22} & \bar{A}_{26} \\ \bar{A}_{16} & \bar{A}_{26} & Q_{66} \end{bmatrix} \begin{Bmatrix} \bar{\epsilon}_x - \bar{\epsilon}_{xN} \\ \bar{\epsilon}_y - \bar{\epsilon}_{yN} \\ \bar{\gamma}_{xy} - \bar{\gamma}_{xyN} \end{Bmatrix} \tag{2}$$

where an overhead bar over a variable is used to denote the laminate parameter. The laminate stiffness A_{ij} can be related to the lamina stiffness Q_{ij} using the classical laminate plate theory

$$\bar{A}_{ij} = \frac{1}{\bar{h}} \sum_{k=1}^{n} Q_{ij}^{(k)} h_k \tag{3}$$

where k represents the kth ply and $\bar{h}$ is the total thickness of the laminate. Plane stress assumption was used for the derivation.

A finite element method with quadrilateral isoparametric elements was used for the modeling. Detail of the derivation has been given in an earlier paper [8] and will not be repeated here. The final form of nodal force-displacement relations is given in the following

$$\{F\} = \int_V [B]^T[Q][B]\{q\}dV - \int_V [B]^T[Q]\{\epsilon_N\}dV \tag{4}$$

where nodal force $\{F\}$, nodal displacement $\{q\}$ and the nonmechanical force vector are 8×1 column matrices and the remaining term is an 8×8 matrix.

4. DAMAGED LAMINA FORMULATION

As given in Reference [8], the effective in-plane constitutive relations of a damaged composite lamina with matrix cracking and fiber breakage can be written in the following form

$$\epsilon_1 = D_1^{-1}S_{11}\sigma_1 + S_{12}\sigma_2$$

$$\epsilon_2 = S_{12}\sigma_1 + D_2^{-1}S_{22}\sigma_2 \tag{5}$$

$$\epsilon_6 = D_6^{-1}S_{66}\sigma_6$$

where lamina coordinates and contracted notation have been assumed. D_1, D_2 and D_6 are the internal state variables representing the damaged state of the lamina. D_1 is the stiffness degradation factor associated with fiber breakage; D_2 and D_6 are the stiffness degradation factors perpendicular to the fiber direction and shear component, respectively, due to matrix cracking. The degraded stiffnesses can be obtained from Equation (5) as

$$E_{11} = D_1E_{11}^{\circ}$$

$$E_{22} = D_2E_{22}^{\circ} \tag{6}$$

$$G_{12} = D_6G_{12}^{\circ}$$

where E_{11}, E_{22} and G_{12} are the effective damaged lamina stiffnesses and E_{11}°, E_{22}° and G_{12}° are the undamaged lamina stiffnesses. In Equations (5) and (6), the internal state variables D_1, D_2 and D_6 are less than unity if damage has occurred in the lamina.

Assumption is made here to simplify the calculation as the case for tensile loading [8]. Here, the internal state variables D_i are treated as material properties (constants) rather than variables depending on the constraint plies. Similar to the tension case, no theoretical study has been done to evaluate the D_1 under compressive loading. It will be determined using a parametric study with one data point, and then it is fixed for the specific material system. Unlike tensile loading, the crack surfaces are not traction free under compressive loading. Therefore, the values of D_1, D_2 and D_6 under compressive loading are expected to be larger than those under tensile loading.

5. FAILURE CRITERIA

In-plane failure can globally be classified into matrix cracking and fiber breakage. A matrix cracking caused by compressive loading may have a different mechanism microscopically than that caused by tensile loading. However, in the problem of progressive failure, it is more important to understand the stress redistribution due to a crack rather than how the crack was generated (by tension mode, compression mode or other modes). A cracked element has different boundary conditions under different loading conditions but does not depend on the failure mode. Therefore, we only need a set of failure criteria that can predict the matrix failure and fiber breakage. A lamina based fiber failure criterion [4,8] has been applied successfully to predict the ultimate strength of composite laminates. It states that

$$\frac{\sigma_1^2}{XX'} + \sigma_1\left(\frac{1}{X} - \frac{1}{X'}\right) = e_f \tag{7}$$

where σ_1 is the stress along the fiber direction and X and X' are the respective tensile and compressive strength of a 0° laminate. When $e_f \geq 1$, the laminate has failed. The application of this failure criterion under compressive loading is based on the fact that a similar failure mechanism has been observed for unidirectional composites and the 0° ply within a multidirectional laminate with a hole [10–15].

The matrix cracking was predicted using the Tsai-Wu quadrilateral failure criterion. In terms of strength ratio, the Tsai-Wu criterion states that

$$[F_{ij}\sigma_i\sigma_j]R^2 + [F_i\sigma_i]R - 1 = 0 \tag{8}$$

when $R \leq 1$, the failure has occurred. Once failure has occurred, either matrix or fiber or both, Equation (5) is used to describe the damaged ply of the element.

6. COMPUTATION PROCEDURES

The finite element meshes used for this study were generated using the computer program "FEMESH" developed in Reference [8]. The program "PROFAS" [8] was then used for the stress and the damage analysis. Different values of internal state variables, D_1, D_2 and D_6 were used under the compressive loading versus the tensile loading. The computation procedures are briefly described in the following:

1. Read the laminate geometry (node number and coordinates) and boundary conditions from the output of "FEMESH" program.
2. Store the element stiffness matrix and nonmechanical force vector in global coordinates.
3. Solve the nodal displacements and strains at the Gaussian points. The laminate and ply stresses are then calculated using laminate plate theory with the constitutive relations given in Equation (5).
4. Examine the damage state of the laminae within all the elements using Equations (7) and (8).

   Then:

   a. If failure does not occur, go back to step 3 with additional load, $p = p + \Delta p$.
   b. When matrix cracking occurs in any lamina, the damaged lamina constitutive relations as shown in Equation (5) are used to recalculate the element stiffnesses, step 2. Then proceed to step 3 with the next load increment, $p = p + \Delta p$.
   c. If fiber breakage is predicted, the distribution and redistribution of the stresses are calculated at the same load level. This step is repeated until no additional damage is detected. Then increase the load and go back to step 2.

5. For fiber dominated laminates, ultimate failure is assumed to occur when fiber breakage has occurred across the entire width (one line of elements) of the laminate.

7. PARAMETRIC STUDIES

The accuracy of the stress-strain distribution calculated with this finite element computer code has been proven very well in an earlier study [8]. The effects of element size and the magnitude of load increment on the strength prediction are discussed in this section. Three representative finite element meshes used for the study in this article are illustrated in Figure 2. The material used for this study is Gr/Ep (graphite/epoxy) AS4/3502 and the elastic and strength properties are given in Table 1.

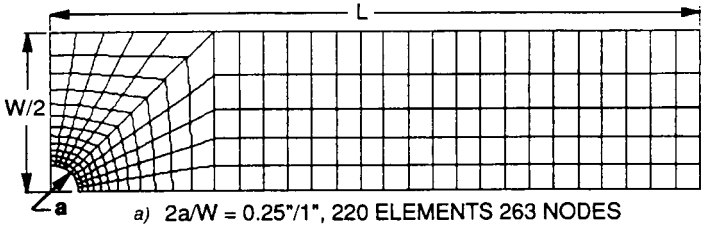

a) 2a/W = 0.25"/1", 220 ELEMENTS 263 NODES

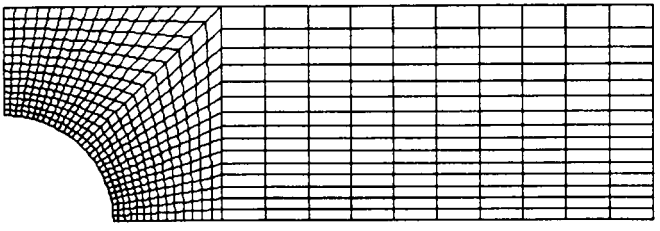

(b) 2a/W = 0.5"/1.0", 570 ELEMENTS 625 NODES

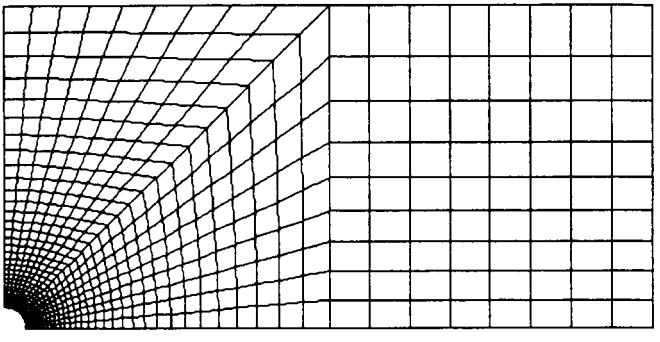

(c) 2a/W = 0.1"/1.5", 648 ELEMENTS 707 NODES

Figure 2. *Representative finite element meshes.*

Table 1. Material properties of AS4/3502 graphite/epoxy laminae.

Parameter	AS4/3502 psi
(a) Elastic Properties	
Longitudinal modulus, E_{11}	20.87×10^6
Transverse modulus, E_{22}	1.72×10^6
Shear modulus, G_{12}	0.97×10^6
Poisson's ratio, ν_{12}	0.326
Longitudinal thermal expansion coefficient, α_1	-0.89×10^{-6}/°C
Transverse thermal expansion coefficient, α_2	23.0×10^{-6}/°C
Temperature change, ΔT	−125°C
Moisture content change, ΔH	0

Parameter	AS4/3502 MPa (ksi)
(b) Strength Properties	
Longitudinal tensile strength, X	270
Longitudinal compressive strength, X'	215
Transverse tensile strength, Y	7.5
Transverse compressive strength, Y'	30
In-plane shear strength, S	9.4

7.1 Effects of Finite Element Sizes

Since the finite element mesh was generated using a mathematic equation, the number of elements generated is inversely proportional to the element sizes. The effects of the internal state variables D_1, D_2 and D_6 have been shown to be very important to the strength prediction under tensile loading [8]. Therefore, their significance under compressive loading was also studied and presented here.

Figure 3 presents the ultimate strength of Gr/Ep $[0/90/\pm 45]_s$ laminates containing a central hole under compressive loading. The hole-to-width ratio ($2a/W$) is 0.3″/1″. The finite element meshes employed here include 42, 162, 272, 400 and 552 elements, and the magnitude of the load increment is −2 ksi. The parameter D_1 varies from 0.001 to 0.15, and D_2 and D_6 range from 0.01 to 0.30. For $D_2 = D_6 = 0.30$, the predicted ultimate strengths are −32 and −46 ksi for D_1 equal to 0.01 and 0.15, respectively. The difference is approximately 44%. This result shows that the ultimate strength is quite sensitive to the stiffness degradation factors. This is attributed to the relaxation of stresses due to micro-damage. Similar rational analysis can be performed for the tension case [8] to support this argument.

7.2 Effects of Load Increment

The effects of the magnitude of load increment were studied using the Gr/Ep $[0/90/\pm 45]_s$ laminates with the opening-to-width ratio $2a/W = 0.3/1.0$. To minimize the possible effects due to the mesh sizes, a relatively fine mesh that con-

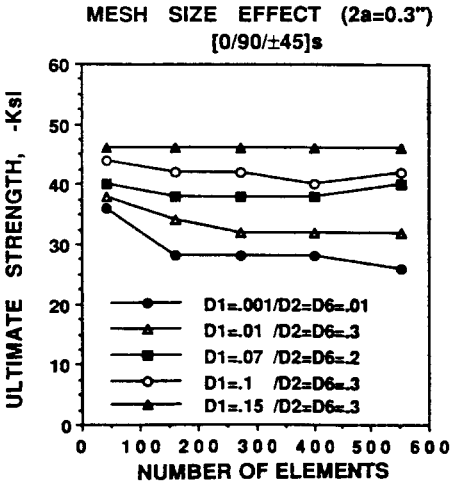

Figure 3. Effects of element size on the ultimate strength of an AS4/3502 [0/90/±45]$_s$ laminate with 2a/W = 0.3 in./1.0 in.

tains 552 elements was used for this study. The steps of load increment (Δs) include -1, -2, -3 and -5 ksi. The result in Figure 4 shows that some predictions with different values of D_1, D_2 and D_6 could be the same when the load increment was as large as -5 ksi. From this study, we suggest that the magnitude of the load increment should not be larger than 3 ksi for fiber dominated

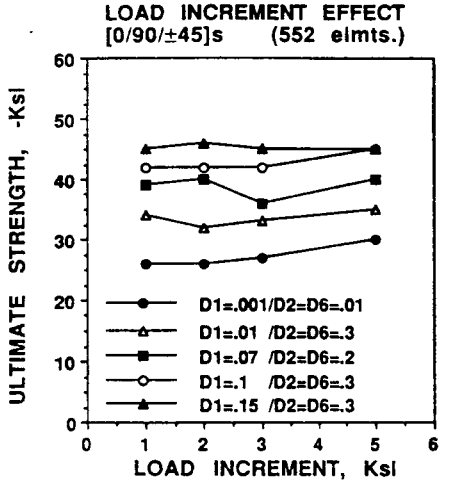

Figure 4. Effects of magnitude of load increment on the ultimate strength of an AS4/3502 [0/90/±45]$_s$ laminate with 2a/W = 0.3 in./1.0 in.

laminates. For the smallest load increment, $\Delta s = -1$ ksi, the predicted ultimate strength for $D_2 = D_6 = 0.30$ and D_1 equal to 0.01 and 0.15 are -34 and -45 ksi, respectively. These results are very close to the predictions using $\Delta s = -2$ ksi in the previous section.

8. RESULTS

The results presented in this article include the predicted ultimate strength and the failure mechanism. The predictions are compared with experimental results.

8.1 Ultimate Strength

The load transferring mechanism of a laminate contains a cracked ply under tensile loading different from that under compressive loading. Under tensile loading, the crack surfaces are traction free, whereas under compressive loading, the crack surfaces can still carry load. Therefore, the stiffness degradation factors D_1, D_2 and D_6 under compressive loading must be higher than those under tensile loading. In the previous work [8], these factors were found to be $D_1 = 0.07$ and $D_2 = D_6 = 0.2$ for AS4/3502 laminates under tensile loading. These values were used in the calculation of compression loading as a baseline solution. Analysis was also made by using $D_1 = 0.14$ and $D_2 = D_6 = 0.4$ that are twice the values for those under tensile loading.

The prediction for the ultimate strength (collapse strength) of AS4/3502 $[0/\pm 45/90]_{2s}$ laminates are compared to the experimental values in Figure 5. The specimens considered have a constant width, $W = 1$ inch. In the case of hole diameter equal to zero, we simply mean unnotched laminates. The result for 1.5 inch wide specimens are illustrated in Figure 6. In both cases, the predictions with $D_1 = 0.14$ and $D_2 = D_6 = 0.4$ agree quite well with the experimental

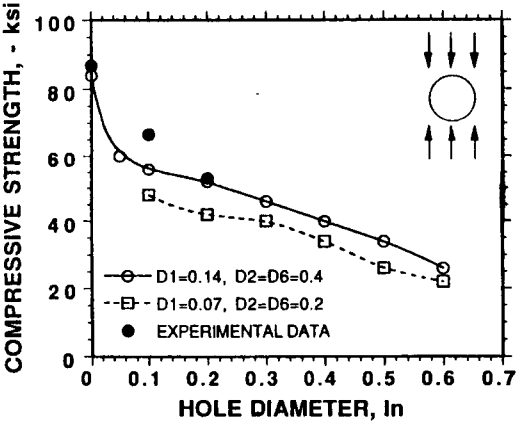

Figure 5. *Predicted and experimental strengths of AS4/3502 $[0/\pm 45/90]_s$ laminates with W = 1 in.*

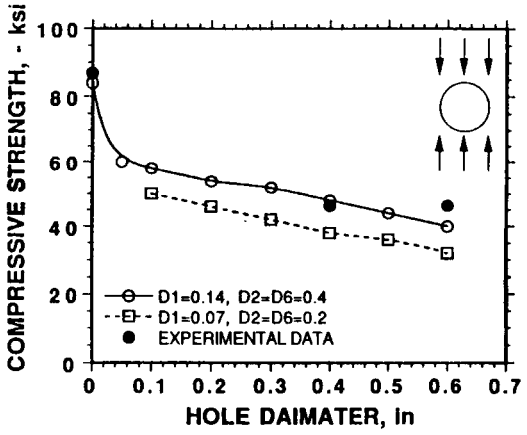

Figure 6. *Predicted and experimental strengths of AS4/3502 $[0/\pm 45/90]_s$ laminates with W = 1.5 in.*

data. The prediction with $D_1 = 0.07$ and $D_2 = D_6 = 0.2$ appears to be too conservative.

Once the stiffness degradation factors are determined, they are assumed constants for the material system and not dependent on the laminate layups. This approach is virtually the same and consistent with the treatment under tensile loading [8]. To further validate this model, another comparison is presented in Figure 7 for AS4/3502 $[0_2/\pm 45]_{2s}$ laminates. The analysis and the experiment were done for 1 inch wide specimens. Their values agree very well. It appears

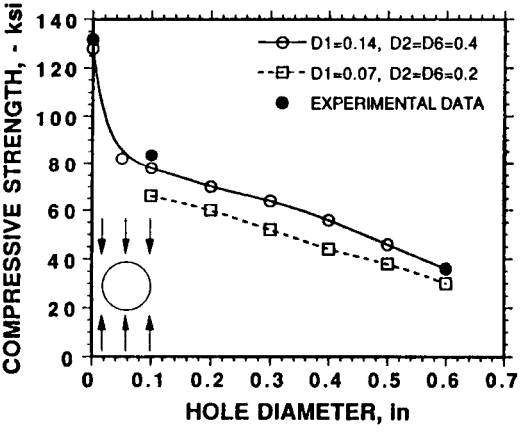

Figure 7. *Predicted and experimental strengths of AS4/3502 $[0_2/\pm 45]_{2s}$ laminates with W = 1 in.*

that the same D_1, D_2 and D_6 can be used for the $[0_2/\pm 45]_{2s}$ laminates, as well as for the $[0/\pm 45/90]_{2s}$ laminates. All the predictions in Figures 5–7 use 500 to 600 elements, except the case of $2a = 0.1$ inch, which uses 702 elements.

8.2 Damage Progression

As we increase the applied load to a critical level, micro-damage will initiate from the hole boundary. This micro-damage includes matrix cracking, fiber matrix splitting, delamination, fiber kinking and microbuckling. They grow as the applied load increases. To examine the capability and accuracy of the present model, two examples are given in the following using AS4/3502 laminates. Figure 8 shows the prediction of a 1.50 inch wide $[0_2/\pm 45]_{2s}$ laminate with a 0.295 inch hole in the center. This finite element mesh contains 150 elements and 180 nodes. At -58 ksi, longitudinal splitting was predicted in the 0° ply (i.e., parallel to the loading direction). Matrix crackings appear in the 45 and $-45°$ plies, and fiber breakage (shear crippling or microbuckling) occurs in the 0° layer. Figure 8(d) gives a superimposed view of Figures 8(a)–8(c).

The X-ray radiograph (with penetrant to enhance the image) in Figure 9 reveals extensive fiber matrix splitting in the 0° layer and fewer matrix crackings in the 45 and $-45°$ plies. The fiber breakage (shear crippling or microbuckling) is clearly shown by the black horizontal line emanating from the hole. The length of the fiber breakage is 0.09 inches, which is slightly shorter than the predicted value, of 0.12 inches.

Ultimate failure is assumed to occur when fiber breakage occurs across the entire width of a layer within a laminate. When we increase the load to -70 ksi (Figure 10), shear crippling was predicted across the entire width of the 0° layer

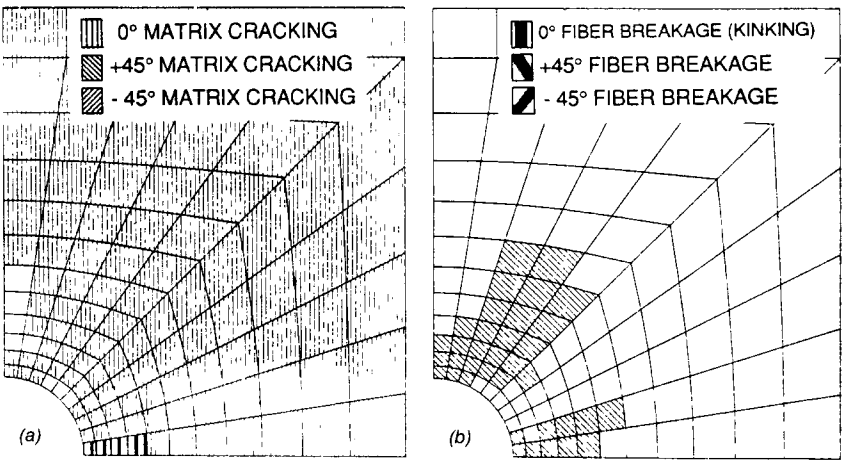

Figure 8. *Predicted damage of a $[0_2/\pm 45]_{2s}$ laminate with 2a/W = 0.295 in./1.501 in. at -58 ksi: (a) 0° ply, (b) 45° ply, (c) $-45°$ ply and (d) superimposed.*

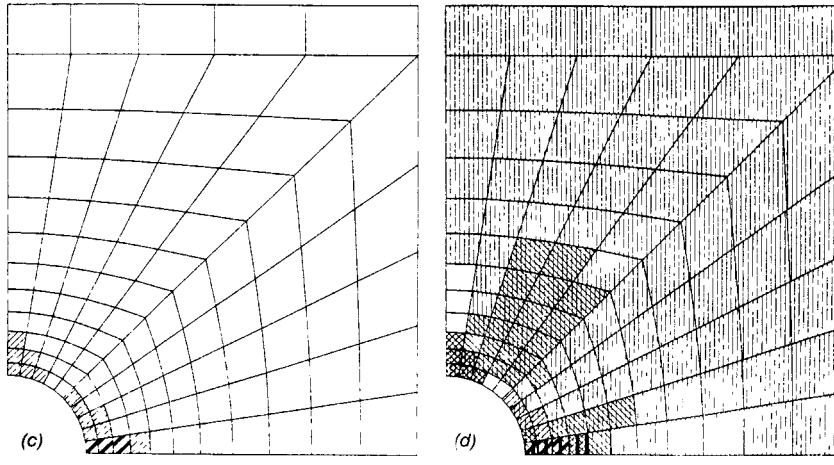

Figure 8 (continued). *Predicted damage of a $[0_2/\pm 45]_{2s}$ laminate with 2a/W = 0.295 in./1.501 in. at −58 ksi: (a) 0° ply, (b) 45° ply, (c) −45° ply and (d) superimposed.*

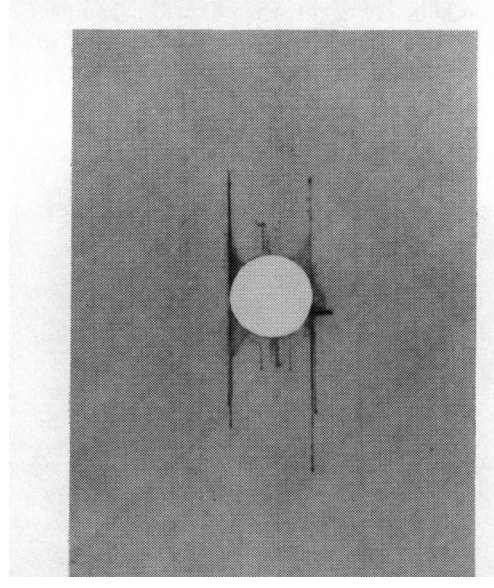

Figure 9. *X-ray radiograph of a $[0_2/\pm 45]_{2s}$ specimen with 2a/W = 0.295 in./1.501 in. after loaded to −57.9 ksi (96% ultimate).*

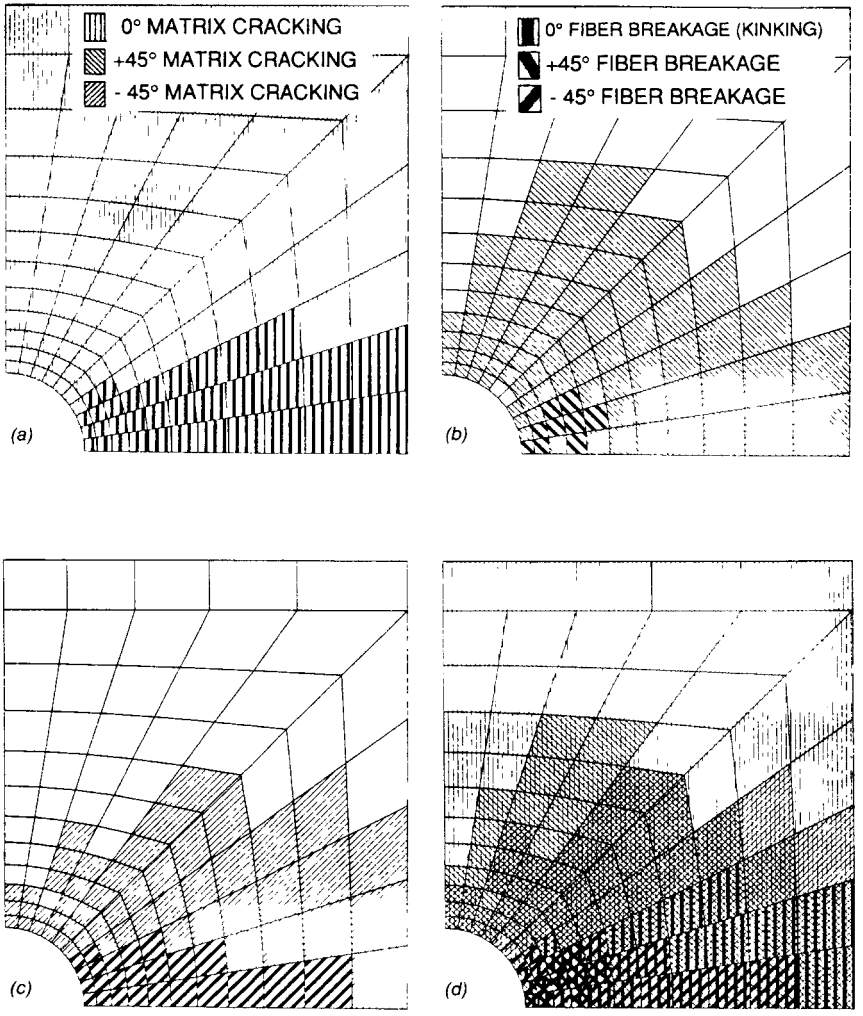

Figure 10. *Ultimate failure of a* $[0_2/\pm 45]_{2s}$ *laminate with 2a/W = 0.295 in./1.501 in. at −70 ksi: (a) 0° ply, (b) 45° ply, (c) −45° ply and (d) superimposed.*

and passes through the hole. Shear crippling was also predicted in the 45 and $-45°$ plies. Extensive matrix crackings appear in all laminae. The experimental value of the ultimate strength of this laminate configuration is -64.2 ksi. Again, the correlation between the prediction and the experiment is good.

9. DISCUSSION AND CONCLUSIONS

The progressive failure model that was developed earlier [8] for laminated composites under tensile loading is extended to compressive loading in this article. The key parameter for this extension and development is the use of the internal state variables D_1, D_2 and D_6. From the consideration of the physical boundary conditions and the load transferred mechanism of a cracked laminate under tensile and compressive loadings, we obtained different values of stiffness degradation factors for different conditions. For AS4/3502 laminates, the values of the D_1, D_2 and D_6 of a damaged ply under compressive loading were determined to be twice those for tensile loading. Although Nuismer and Tan [16] have pointed out that internal state variables are laminate dependent, they were assumed to be independent of laminate layups in this study to reduce the complexity of the problem. Comparisons were made with experimental data for the AS4/3502 $[0/\pm 45/90]_{2s}$ and $[0_2/\pm 45]_{2s}$ laminates (Figures 5-7). Good agreement was obtained using constant values of the stiffness degradation factors, $D_1 = 0.14$ and $D_2 = D_6 = 0.4$.

The damage progression was studied using an AS4/3502 $[0_2/\pm 45]_{2s}$ laminate with hole-to-width ratio equal to 0.295″/1.501″. At -58 ksi, microbuckling was predicted, in addition to longitudinal splitting in the 0° layer (Figure 8). This predicted failure mechanism agrees reasonably well with the X-ray radiograph, as shown in Figure 9.

This model is not as complicated as some other models in the literature. However, it is promising because its accuracy has been verified by experimental data. Following the same approach, other types of loading conditions should be applicable as well. At the present time, this model does not take into account delamination that could occur around the hole. Additional study is needed for laminates that exhibit extensive delamination around the hole.

REFERENCES

1. Nuismer, R. J. and J. D. Labor. 1979. "Applications of the Average Stress Failure Criterion: Part II—Compression," *J. Composite Materials*, 13:49-60.
2. Rhodes, M. D., M. M. Mikulas, Jr. and P. E. McGowan. 1984. "Effects of Orthotropy and Width on the Compression Strength of Graphite-Epoxy Panels with Holes," *AIAA Journal*, 22:1283-1292.
3. Tan, S. C. 1987. "Tensile and Compressive Notched Strength of PEEK Matrix Composite Laminates," *J. of Reinforced Plastics and Composites*, 6:253-267.
4. Tan, S. C. 1988. "Effective Stress Fracture Models for Unnotched and Notched Multidirectional Laminates," *J. Composite Materials*, 22:322-340.
5. Nuismer, R. J. 1978. "Continuum Modeling of Damage Accumulation and Ultimate Failure in Fiber Reinforced Laminated Composite Materials," *Research Workshop on Mechanics of Composite Materials, ARO and NSF*, pp. 55-77.

6. Chou, S. C., O. Opringer and J. H. Rainey. 1977. "Post-Failure Behavior of Laminates: II—Stress Concentration," *J. Composite Materials,* 11:71–78.
7. Irvine, T. B. and C. A. Ginty. 1986. "Progressive Fracture of Fiber Composites," *J. Composite Materials,* 20:166–184.
8. Tan, S. C. 1991. "A Progressive Failure Model for Composite Laminates Containing Openings," *J. Composite Materials,* 25:556–577.
9. Chang, F. K. and L. B. Lessard. 1991. "Damage Tolerance of Laminated Composites Containing an Open Hole and Subjected to Compressive Loadings: Part I—Analysis," *J. Composite Materials,* 25:2–43.
10. Starnes, J. H., Jr. and G. Williams. 1982. "Failure Characteristics of Graphite-Epoxy Structural Components Loaded in Compression," *Proceedings of the IUTAM Symposium on Mechanics of Composite Materials, Blacksburg, VA, August 16–19,* Z. Hashin and C. T. Herakovich, eds.
11. Sohi, M. M., H. T. Hahn and J. G. Williams. 1987. "The Effect of Resin Toughness and Modulus on Compressive Failure Modes of Quasi-Isotropic Graphite/Epoxy Laminates," *Toughened Composites, ASTM STP 937,* Norman J. Johnston, ed., Philadelphia, PA: American Society for Testing and Materials, pp. 37–60.
12. Guynn, E. G. and W. L. Bradley. 1989. "A Detailed Investigation of the Micromechanisms of Compressive Failure in Open Hole Composite Laminates," *J. Composite Materials,* 23:479–504.
13. Waas, A. M. and C. D. Babcock, Jr. 1989. "An Experimental Study of the Initiation and Progression of Damage in Compressively Loaded Composite Laminates in the Presence of a Circular Cutout," *Proceedings of the AIAA/ASME/ASCE/AHS/ASC 30th Structures, Structural Dynamics and Materials Conference,* paper no. 89-1274-CP, pp. 1000–1011.
14. Soutis, C. and N. A. Fleck. 1990. "Static Compression Failure of Carbon Fibre T800/924C Composite Plate with a Single Hole," *J. Composite Materials,* 24:536–557.
15. Soutis, C., N. A. Fleck and P. T. Curtis. 1991. "Hole-Hole Interaction in Carbon Fibre/Epoxy Laminates under Uniaxial Compression," *Composites,* 22:31–38.
16. Nuismer, R. J. and S. C. Tan. 1988. "Constitutive Relations of a Cracked Composite Lamina," *J. Composite Materials,* 22:306–321.